3 SPATIAL DISTRIBUTION OF CODA SCATTERERS

3.1 INTRODUCTION

The fundamental assumption of all coda models of Chapter 2 is that intrinsic absorption and the distribution of structures causing scattering is random and uniform (e.g. Aki & Chouet, 1975 [9]; Sato, 1977 [18]). As a result of this assumption all these models predict that the envelopes of S coda waves should decay smoothly and that the coda decay rate should be independent of the hypocenter. The observed envelopes of S coda waves differ from those synthesized by models based on the hypothesis of a random and uniform distribution of scatterers in space. Small amplitude fluctuations or ripples overlying on a smoothly decaying coda envelope which is predicted by the scattering theory, are often observed. This observed behaviour can be explained by a non-uniform three-dimensional distribution of scatterers in the crust due to localized inhomogeneities such as active faults, volcanoes, subducting slabs and so on. Then, a deterministic approach on coda waves is necessary in order to elucidate the detailed inhomogeneous structures in the crust and the upper mantle.

Nishigami (1991) [40], identified the structures causing strong scattering by analyzing the observed coda envelope fluctuations from a synthesized model. In this work, he analyzed the seismic data of Hokuriku district of central Japan and detected zones of strong scattering in the surface layer and upper crust; some of these regions of strong scattering were located near major active faults. Applying the coda-envelope-inversion technique to three regions in central part of Japan, Nishigami [41] identified significant heterogeneous structures in the crust around one active fault system and two active volcanoes. In the same way, he established also the three-dimensional distribution of scatterers in the crust in San Andreas Fault system region [42]. There are also other authors applying similar techniques to other regions. Chen and Long (2000) [43], in the Piedmont Province of central Georgia, found a correlation at shallow depths between zones of strong scattering and the location of hypocenters and areas with greater topographic relief, and were able to identify a strong reflecting layer which was consistent with a thrust plain previously reported using other geophysical methods.

More recently, Asano and Hasegawa (2004) [44] suggested the correlation between large scattering zones with the existence of fault-damaged zones in south-western Japan, as well as other scattering properties of the region at different depths.

Following Nishigami's work, in section 3.2, we will develop the method of analysis necessary to establish the distribution of scatterers. This method implies a previous knowledge of the depth dependent velocity model and it assumes a synthetic single isotropic scattering model for the absolute reference scattering coefficients (Sato, 1977, [18]). An important step to establish this distribution is the computation of the energy residuals. This calculation is explained in detail in section 3.3.

3.2 THE OBSERVATIONAL EQUATION

In this section, we are going to develop an inversion method of coda waveforms in order to estimate the spatial distribution of coda scatterers deterministically. Therefore we will derive the relationships between the fluctuation of observed coda power envelope and the spatial variation of scattering coefficient.

We start by considering the Single Isotropic Scattering (SIS) model for the shape of the coda of local earthquakes [18] which assumes single isotropic scattering, random and homogeneous distribution of scatterers, and spherical radiation of elastic energy. According to the SIS model, and considering the anelastic attenuation effect, the coda energy density at a frequency f, hypocentral distance r and lapse time t in a three-dimensional space can be expressed as an integral all over the space in the form [18]:

$$E_s(f \mid r,t) = \int_V \frac{W_0(f)g(f)}{(4\pi)^2\,\beta\; r_1^2 r_2^2}\, \mathrm{e}^{-2Q_c^{-1}\pi f t}\, \delta\left[t - \frac{r_1 + r_2}{\beta}\right] \mathrm{d}V \qquad (3.1)$$

where $\mathrm{d}V = \mathrm{d}^3x$; $\mathbf{x}$ is the coordinate vector of the scattering point; $r_1 = |\mathbf{x}|$ is the distance between the hypocenter and the scatterer; $r_2 = |\mathbf{x} - \mathbf{r}|$ is the distance between the scatterer and the station; $r = |\mathbf{r}|$; t is the lapse time measured from the origin time of the earthquake; β is the average S-wave velocity; $W_0(f)$ represents the total energy radiated from the source within a unit frequency band around f; and $g(f)$ is the total

scattering coefficient for the frequency *f*. In a constant velocity medium, the scatterers responsible for the generation of coda waves at a distance *r* and time *t* are contained in a spheroidal shell whose foci are located at the source and receiver, which is expressed by the term $(1/\beta)\delta\left[t-(r_1+r_2)/\beta\right]$ in Eq. (3.1). The integration of Eq. (3.1) gives [18]

$$E_s(f\,|\,r,t)=\frac{W_0(f)\,g_0(f)}{4\pi r^2}\,K(a)\,\mathrm{e}^{-2Q_c^{-1}\pi f t} \tag{3.2}$$

for a homogeneous spatial distribution of the scattering coefficient $g_0(f)$, being $K(a)=(1/a)\ln\left[(a+1)/(a-1)\right]$ for $a>1$; $a=t/t_S$; and t_S the S-wave travel time. For $a>>1$ $K(a)\approx 2/a^2$ and therefore Eq.(3.2) becomes

$$E_s(f\,|\,r,t)\approx\frac{W_0(f)\,g_0(f)}{2\pi\beta^2 t^2}\;\mathrm{e}^{-2Q_c^{-1}\pi f t},\quad (t>2t_S) \tag{3.3}$$

which corresponds to the single scattering model of Aki and Chouet (1975) [9].

We divide the area under consideration into a number *N* of small blocks of volume δV, as it will be detailed later. Therefore, by multiplying the right side of Eq. (3.1) by the factor 1/2 for including the effect of a half space, then by integrating Eq. (3.1) in the radial direction over the spheroidal shell (which radius is approximated by $\beta t/2$), which corresponds to the lapse time window $t_j\pm\delta t/2$ (the magnitude of δt will be computed in section 3.3), we obtain:

$$E_{sa}(f\,|\,t_j)\delta t\approx\frac{W_0(f)\,g_0(f)}{4\pi^2\beta t}\;\mathrm{e}^{-2Q_c^{-1}\pi f t_j}\sum_{i=1}^{N_j}\frac{\delta_{ij}}{\left(r_{1,i}r_{2,i}\right)^2}\delta V \tag{3.4}$$

where the integral has been approximated by a summation of the blocks, where each term corresponds to a certain block *i*. The sub index *a* in the energy density indicates the consideration of an average scattering coefficient g_0 over the half space. δ_{ij} equals 1 when the *i*th block lays inside the spheroidal shell which corresponds to the *j* time window and equals zero otherwise. N_j is the total number of scatterers in each spheroidal shell.

The observed coda envelope fluctuations from the theoretical model due to the

non-uniform distribution of scatterers can be expressed mathematically as spatial perturbations of the average scattering coefficient of the medium due to an individual scatterer in the form: $g=g_0\alpha_i$ ($\alpha_i \geq 0$). Thus, the integration of Eq.(3.1) gives:

$$E_s(f \mid t_j)\delta t = \frac{W_0(f)\, g_0(f)}{4\pi^2 \beta t}\ \mathrm{e}^{-2Q_c^{-1}\pi f t_j} \sum_{i=1}^{N_j} \frac{\alpha_i \delta_{ij}}{\left(r_{1,i} r_{2,i}\right)^2} \delta V \tag{3.5}$$

To obtain Eq.(3.4) and Eq. (3.5) we have assumed a constant value of Q_c in the region, thus neglecting the effect of an spatial variation of Q_c on the fluctuations of the coda envelope and considering that they are caused mainly by the spatial variations of the scattering coefficient. In order to get a system of equations that will allow us to estimate the spatial perturbations of the scattering coefficient we divide Eq.(3.5) by Eq. (3.4),

$$\frac{E_s(t_j)}{E_{sa}(t_j)} = \frac{1}{\sum_i \frac{\delta_{ij}}{(r_{1,i} r_{2,i})^2}} \sum_i \frac{\alpha_i \delta_{ij}}{(r_{1,i} r_{2,i})^2} \tag{3.6}$$

where the left side of equation Eq. (3.6) is called coda wave energy residual (e_j) and it measures the ratio of the observed energy density in this part of the coda to the average energy density of the medium.

If we divide the coda of one seismogram into several small time windows, we will have one equation based on Eq. (3.6) for each time window. Also for each time window, the scatterers contributing to the energy density are contained in a spheroidal shell. Thus, equation Eq.(3.6) can be re-written in the following form:

$$\begin{aligned} &w_{11}\alpha_1 + \cdots + w_{i1}\alpha_i + \cdots + w_{N1}\alpha_N = e_1 \\ &\vdots \\ &w_{1j}\alpha_1 + \cdots + w_{ij}\alpha_i + \cdots + w_{Nj}\alpha_N = e_j \\ &\vdots \\ &w_{1M}\alpha_1 + \cdots + w_{iM}\alpha_i + \cdots + w_{NM}\alpha_N = e_M \end{aligned} \tag{3.7}$$

where M is the total number of equations (number of seismograms multiplied by the number of coda time windows considered), N is the total number of scatterers (number

of small blocks into which the study region is divided) and

$$w_{ij} = \frac{1}{\sum_i \frac{\delta_{ij}}{(r_{1,i} r_{2,i})^2}} \frac{\delta_{ij}}{(r_{1,i} r_{2,i})^2} \tag{3.8}$$

Solving Eq. (3.7) will provide us the scattering coefficient distribution. The methods to solve such a system of equations will be developed in Chapter 4.

3.3 COMPUTATION OF THE ENERGY RESIDUALS

We will explain now in detail how to compute the energy residuals from the vertical component of seismograms. The steps to follow are:

i. Extraction of frequency components from a certain frequency band, i.e, 4-10 Hz. This is done by using a Butterworth or Chebyshev band-pass filter. The filter has to be applied both forward and backward along the time axis to cause no phase delay. We generated the algorithm to apply the filter by means of the software provided by Tony Fisher [45] in his web page. This web page is a tribute to him (he died on February 29th, 2000).

ii. Computation of the rms amplitudes $A_{\text{obs}}(f \mid r,t)$ of the filtered traces using a time window for the averaging of about ten times the central period of the filter used [73]. The rms amplitudes for a noise window of 10 s before the P-wave arrival are also computed and only the amplitudes greater than two times the signal to noise ratio are kept.

iii. The amplitudes are then corrected for geometrical spreading by multiplying by t^2 which is valid for body waves in a uniform medium.

iv. The average decay curve is estimated for each seismogram by means of a least-squares regression of $\ln\left[t^2 A_{\text{obs}}\left(f \mid r,t\right)\right]$ vs. t and only the estimates with a correlation coefficient greater than 0.70 are kept. It is convenient to consider starting lapse times from about 1.5-2 times [17] the arrival time of the S wave in

order to increase the resolution near the source region .

v. The observed coda residuals $e(t)$ are then calculated by taking the ratio of the corrected observed amplitudes to the estimated exponential decay curve.

vi. We would like to obtain a limited number of coda residuals. So finally the residuals are averaged in time windows of δt to get e_j at discrete lapse times t_j. There is an important reason for this: we will compute the scattering coefficient for each block into which the study region id divided, and every block has a finite volume V. Then, the residuals should correspond to the energy scattered by a finite volume. If a wave takes a certain time to travel the volume $\delta\tau \simeq 2(\delta V)^{1/3}/v$ (the factor 2 comes from considering the wave going back and forth during the scattering process) then we will consider only a certain number of residuals $E(t_j)$ coming from the average of $e(t)$ in a time interval $\delta(t)$ centered at a discrete lapse time t_j. $\delta(t)$ has to be similar but smaller than $\delta(\tau)$ and we consider $t_{j+1} - t_j = \delta(t)$.

All this process is illustrated in Figure 3-1 (for the 4-8 Hz frequency band) and (E)

Figure 3-2 (for the 8-12 Hz) where we show the following: Figures (A) corresponds to a coda waveform of an earthquake at an epicentral distance of 1.91 km and 1.53 km respectively, under Galeras volcano (Colombia). Figures (B) correspond to the band-pass filtered coda waveform of seismograms on figures (A). Figures (C) corresponds to the power spectrum of figures (A). Figures (D) correspond to the logarithm of the running mean-squared amplitudes corrected for geometrical spreading effect. The continuous cyan line is the best linear fitting function to the logarithmic trace. Finally, figure (E) corresponds to the logarithm of the coda energy residuals averaged in a time window of 0.5 s.

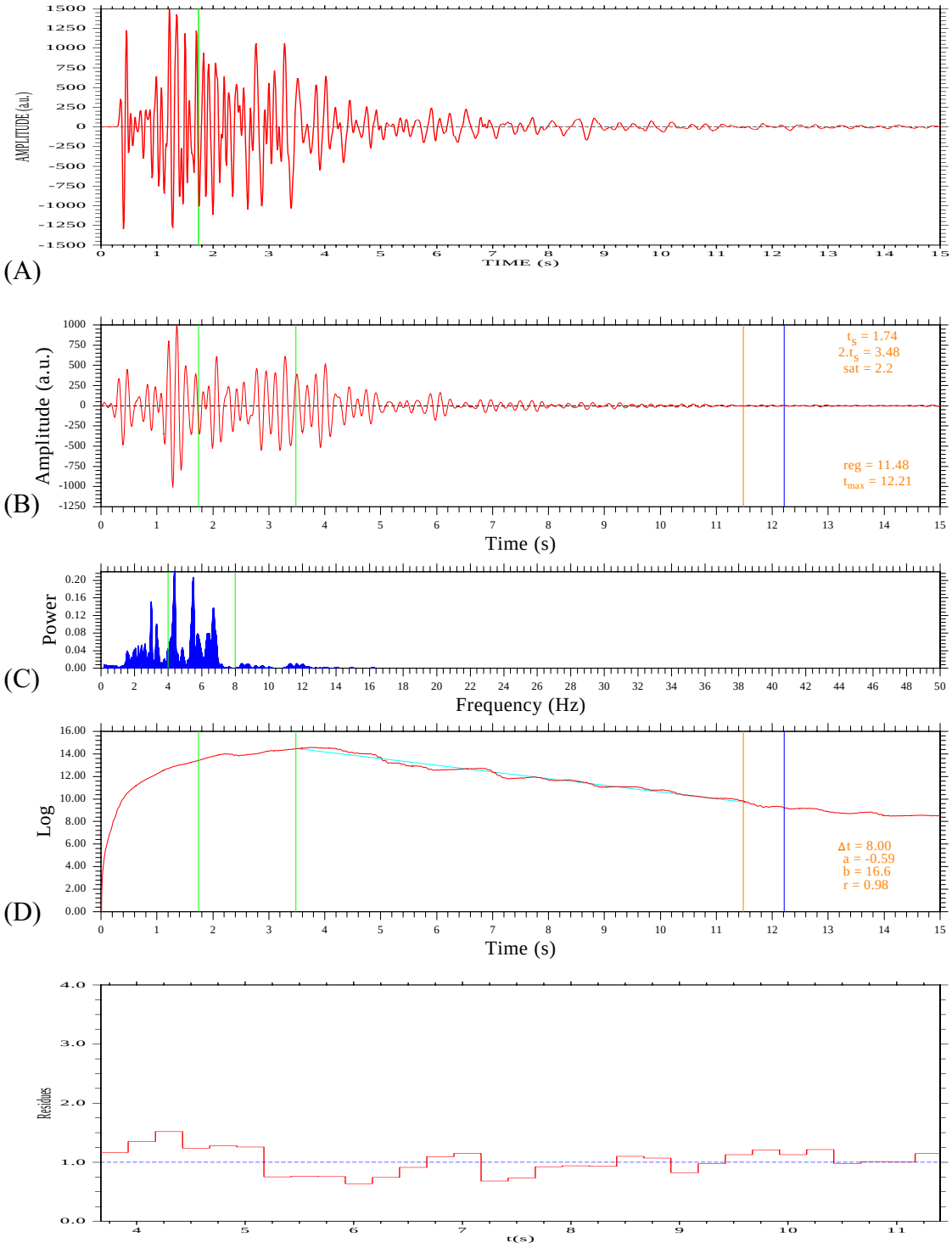

Figure 3-1. Analysis of event 300 recorded by the station 14 in the Galeras volcano (see appendix A). (A) corresponds to the raw seismogram. (B) corresponds to the filtered seismogram in the 4-8 Hz band. (C) is the power spectrum of the seismogram between t=3.48 s and t=11.48 s. This lapse time corresponds to the one that will be used to carry out the linear regression in figure (D). First green line indicates t_s in Figs (A-B-D) and second green line indicates $2t_s$ in Figs (B-D). In Fig (C) green lines indicate the frequency band under analysis. (E) corresponds to the logarithm of the coda energy residuals averaged in a time window of 0.5 s.

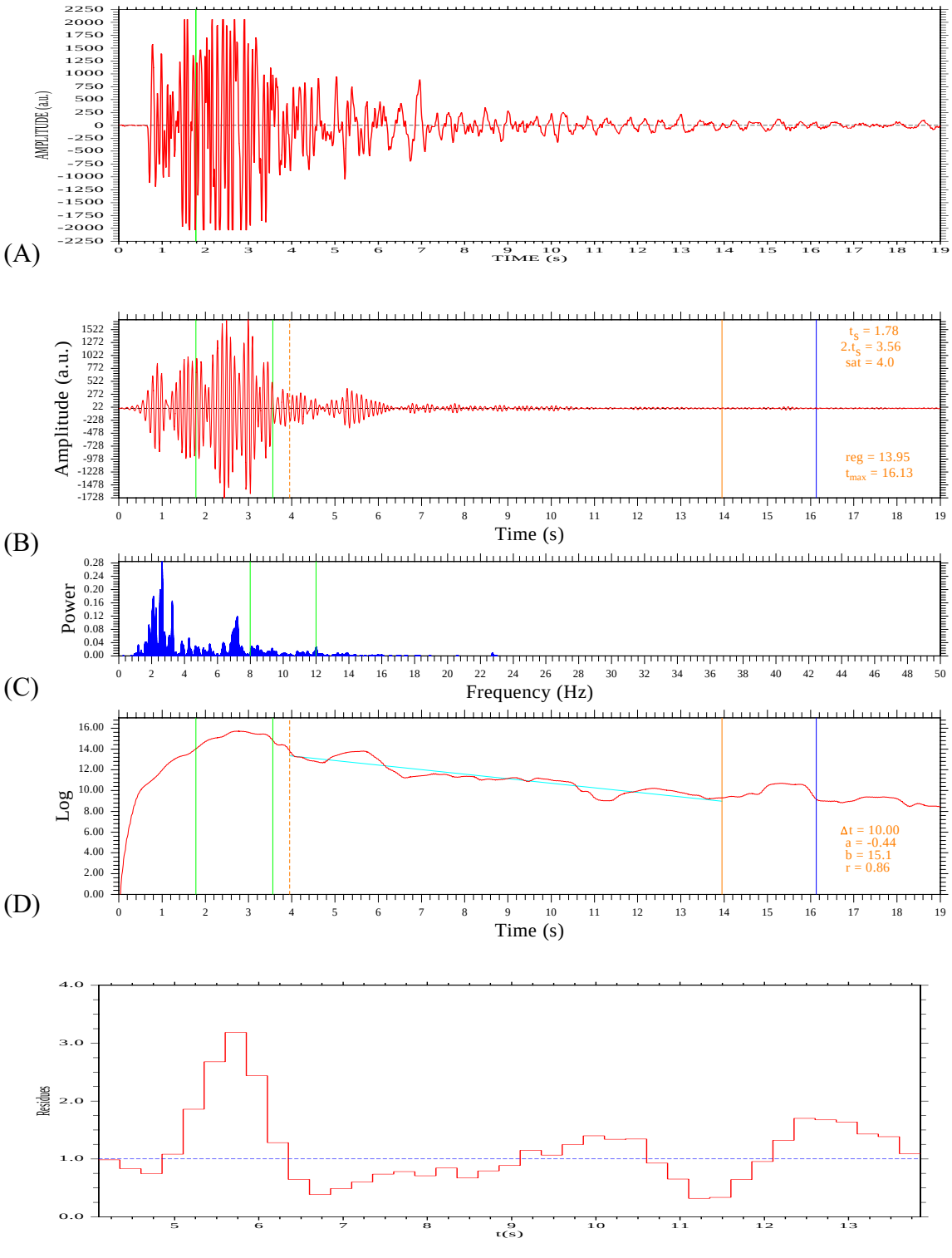

Figure 3-2. Analysis of event 128 recorded by the station 14 in the Galeras volcano (see Appendix A). (A) corresponds to the raw seismogram. (B) corresponds to the filtered seismogram in the 8-12 Hz band. (C) is the power spectrum of the seismogram (A) between t=4.0 s and t=13.95 s. This lapse time corresponds to the one that will be used to carry out the linear regression in figure (D). First green line indicates t_s in Figs (A-B-D) and second green line indicates $2t_s$ in Figs (B-D). In Fig (C) green lines indicate the frequency band under analisys. Dashed line indicates a safe initial time to avoid side effects from saturation of the recorded seismogram. (E) corresponds to the logarithm of the coda energy residuals averaged in a time window of 0.5 s.